HARDWARE IMPROVEMENTS ON THE TWO CERN LSD SYSTEMS

CERN-LSD Group (presented by E. Rosso)

INTRODUCTION

The different methods to check the status of the machine are the following :

1) The on-line test program STEP and RAVEN etc. (ref. 1)
2) The output of the calibration program SCALP (ref. 2)
3) The statistical effects in the production.

These investigations have led us to a series of conclusions and this paper describes the different improvements which have been implemented on LSD 1 whenever possible or on LSD 2 whenever a long study or careful checks have been necessary.

We shall limit ourselves to discuss the improvements in the mechanics and in the electronics, the optics developments have been presented in another paper (ref. 3).

1. MECHANICS IMPROVEMENTS

1.1 Machine Alignment

Due to the fact that the machine framework is made of welded iron plates, a correct alignment is a critical operation : this problem is much easier to solve in the case of cast iron blocks. However, to make these ineherent misalignment tolerable, we have taken at CERN the following steps.

a) Periscope and periscope motor have been coupled by means of a knee-cap.
b) A certain amount of backlash has been allowed between the cone and the θ encoder. For this reason the star cotter system (which blocked the two items rigidly) has been discarded and a single cotter system introduced, which allows an easy re-alignment of the cone-encoder axes.

However, we noticed that even if the alignment of the axes is made with the utmost measurable precision, after about 2000 hours of operation, the remaning mis-alignment has caused either :

α) θ error, due to the azimuthal backlash between the cotter and the encoder housing, or, if the cotter is too rigid in the cotter slot,
β) The coming into contact of the two glass discs, due to a stress between fixed and rotary parts of the encoder

In order to eliminate these troubles, we use an elastic cotter which allows a slight radial movement without azimuthal backlash.

1.2 Cone-periscope system on LSD 2.

Let us remind that cone and periscope on LSD 1 have been manufactured using "Anticorodal" blocks, thermically stabilized, rectified and hardened by an oxydizing treatment : the periscope was guided by a metal bushing.

To obtain more robustness and less friction for the second machine, we used iron blocks and a slide gear system which assures a backlash free guidance of the periscope.

1.3 Adjustable slit position on LSD 2.

Analysing the RAVEN displays and the colibration results on LSD 1, we realized (Ref. 4) the importance of accuratly positioning the slit. So we supplied the LSD 2 with an adjustable slit support.

1.4 Adjustement of the periscope linear encoder position.

On LSD 2 we installed a new linear encoder and reference mark system : both gratings are carried by the same strip of glass. So, in order to adjust the value of the R_o parameter (which plays an important role in the calibration (ref. 5), we have mounted the Heidenhain head on a vertical high precision slide-rail, controlled by mycrometic screws (fig. 1).

1.5 Periscope linear potentiometer.

A linear potentiometer, mounted on the periscope, is used by the manual periscope position servo and the AGC circuit. Fig. 2 shows an elastic mechanical element which allow, without damaging the potentiometer, a further movement of the periscope even if cursor reaches its lower limit.

2. ELECTRONICS IMPROVEMENTS

2.1 Noise.

The greatest troubles we had on LSD 1 were connected with the superimposition of noise to the measurement pulses. So we studied in detail the different effects of the noise, its sources and the possibilities to eliminate them.

2.1.1 Principal effects of noise

The pulse analysis system is closely derived from the Berkeley design (Ref. 6). However, the valid pulse criterion, based on the number of digital steps counted before and

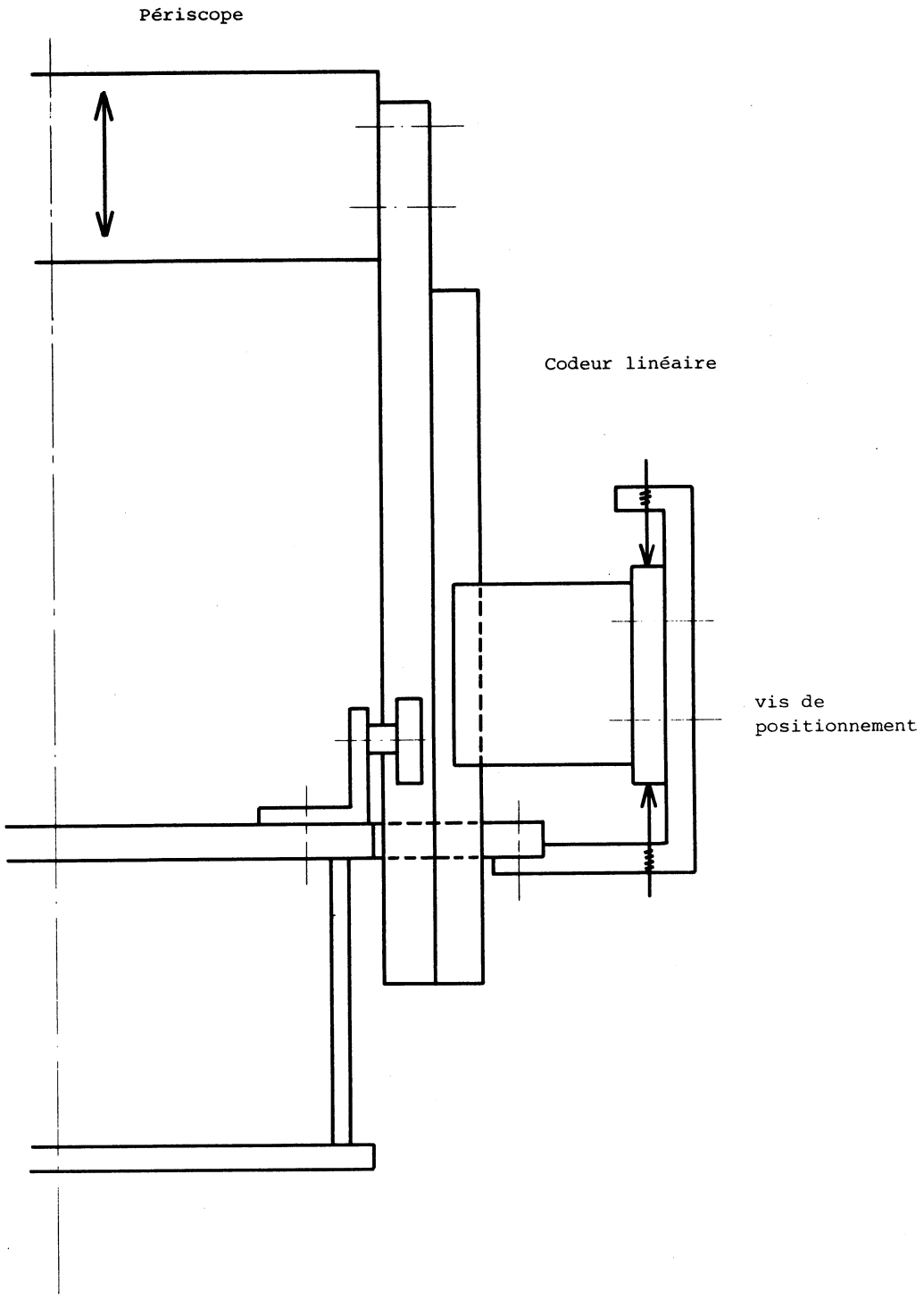

Fig. 1

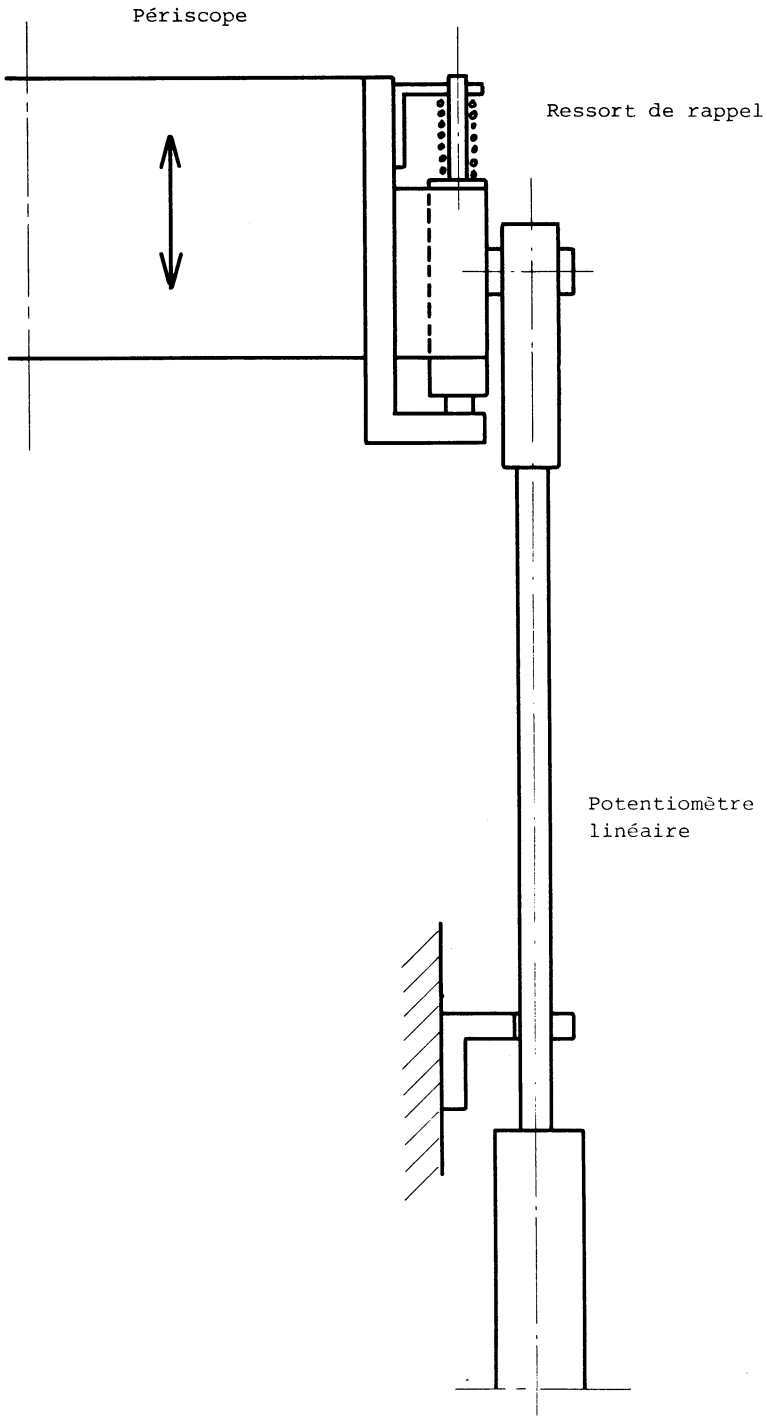

Fig. 2

after the pulse top, consists of 5 up-3 down OR 3 up-5 down (instead of 5 up-5 down). The noise presence causes the following effects :

a) The θ coordinate, if we measure it at 1 step from the top (LSD 1), may be wrong if the noise level exceeds 1 step (150 mV) (fig. 3).
b) Due to the fact that the up (respect. down) counter is reset by each down (respect. up) count, we might loose good pulses, particularly those having a small pulse height (6-7 counts).
c) In the cone plane, the image of the sides of the film gate is not completely dark, due to the presence of shifted ghost image (ref. 3).

Since the light intensity of the ghost image is in the order of a few percent of the directly projected image, the AGC attempts to normalise the noise. Thus a lot of spurious digitizing are created.

2.1.2 Noise sources.

The total noise is attributable to several noise sources :

a) Schottky noise of the photomultiplier (PM)
b) Secondary emission in the photomultiplier.
c) Spurions pulses, which are induced in the cable connecting PM and VA.
d) Thermal noise of the electronic components.
e) Noise from the ground of the common power supplies.
f) Induced noise from ground loops.
g) Induced noise from parasitic fields acting on electronic circuits.

2.1.3 Means to overcome the noise.

2.1.3.1 Filter systems

The first attempt to extract the useful pulses out of the noise was made by an electronic filter circuit (Ref. 7).

It happened that at small radii already the filter delayed, due to its RC time constant, the useful pulses. It was not possible to correct this delay effect entirely by software corrections. At large radii the equivalent frequencies of the pulses are in the range of the noise frequencies and it was thus, by principle, impossible to filter out the useful pulses.

Thus the efforts to reduce the noise figures were controled on the principal noise sources as mentioned under 2.1.2.

2.1.3.2 Several ways to reduce the noise.

a) Schottky noise was appreciably reduced by using a photomultiplier with appropriate photocathode (S-20) and by using newly developed types of splitting mirrors (see the previous paper).

R = constant

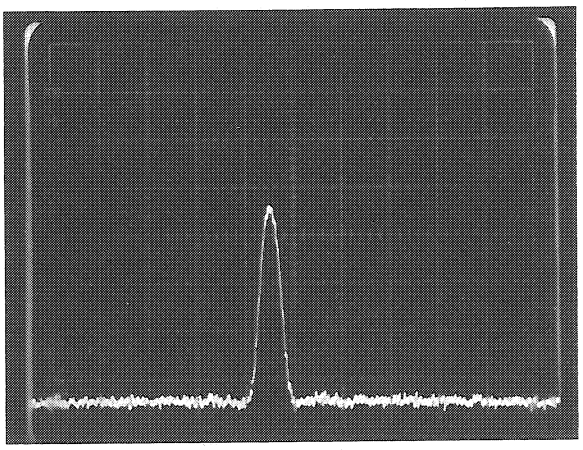

α = 0°

0.1 ms/cm

0.5 V/cm

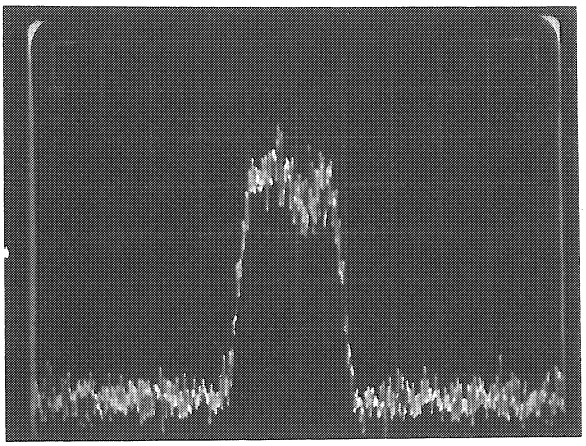

α = 20°

0.1 ms/cm

0.1 V / cm

Fig. 3

b) The effect of secondary emission of the first dynodes of the dynode chain was reduced by the application of the highest possible voltages, stabilized by Zener diodes.
c) Voltage divider network and video-amplifiers were put into the PM housing directly to provide the shortest possible connections. This enables to normalize the pulses prior to their transfer over relatively long cables. However, the AGC circuit has been installed very close to the video-amplifier.
d) Advancement in the state-of-the-act of integrated circuits allows a wider choice in the field of the low-noise operational emplifiers.
e) Each analog circuit cord is equipped with its own power supply. Transfer of analog signals to the logic circuits is done by means of differential amplifiers with high common mode rejection ratio.
f) Ground loops have been avoided by connecting all ground lines to a common ground point in a star-like manner.
g) All analog circuits including the analog to digital converter (ADC) were carefully shielded.

All the corrections mentioned have been applied to LSD 2, while LSD 1, working with a simple Sin^2-filter, got only those improvements mentioned under c),d),e) and f). The output signals of the VA, shown in fig. 4, allow to assess the improvements obtained on both machines.

2.2 Analog circuits developement

2.2.1 AGC circuits

The pulse height of the VA output signal is affected by variations of backround density on the film, which are essentially due to :

a) Uneven illumination of the film
b) Partial azimuthal polarization around the optical axis
c) Uneven illumination of the chamber

The AGC has been especially designed to eliminate these effects. The basic operation carried out by both AGC circuits, may be described as the calculations of the signal-to-backgroudn ratio (see fig. 5).

The aim to obtain (for a given radial track) the relation

$$\frac{I_1}{F_1} = \frac{I_2}{F_2} = \text{const.} \qquad (1)$$

The AGC perfroms the above division and outputs analog signal. Relation (1) means that the AGC correct only linear variations between the VA pulse height and the backround amplitude.

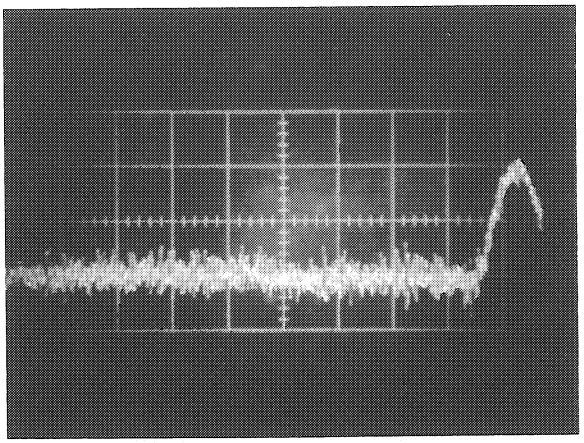

LSD1
PM : XP1110
0.2 ms/cm
1V/cm
Old configuration

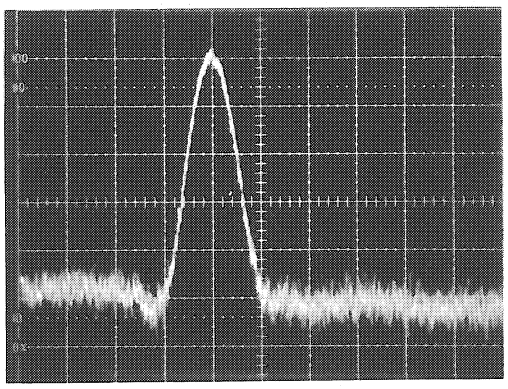

LSD2 and
LSD1 new configuration
PM : XP1110
0.2 ms/cm
0.5V/cm

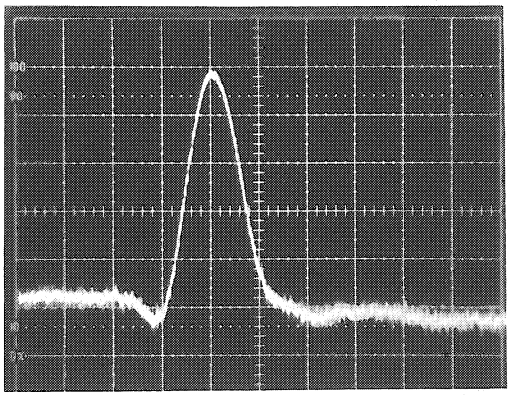

LSD2
PM : XP1002
0.2 ms/cm
0.5V/cm

Fig. 4

Until now, two non linear effects have been detected :

i) A spurious light may come onto the slit. It could be generated either by light sources other than the xenon lamp or by diffraction of tracks on the film.

ii) The optical density of bubbles or backround on the film does not lie on the linear portion of the curve in the plot film density versus logarithm of the exposure (fig. 6).

Let us remind the following definitions :

a) Film optical transmission is given by the ratio of the light passing through the film to the light incident on the film.

b) Film optical density.

c) Film exposure E is the incident energy per unit surface.

Let us define a radial particle track.

A_s the total slit area

A_b the slit area covered by bubbles.

Consider two different illumination conditions :

Condition 1.

Backround : exposure $E_{f1)}$ transmission $T_{f1)}$ and, from b), density $D_{f1} = - \lg T_{f1}$

Bubbles : exposure E_{b1}, transmission T_{b1}, density $D_{b1} = - \lg T_{b1}$

The ratio of the signal amplitude I_1 to the backround amplitude F_1 may be expressed as :

$$\frac{I_1}{F_1} = \frac{A_b\, T_{b1} + (A_s - A_b)\, T_{f1}}{A_s\, T_{f1}} = \frac{A_b\, (T_{b1} - T_{f1})}{A_s\, T_{f1}} + 1 \qquad (2)$$

Condition 2.

Backround : exposure E_{f2}, transmission T_{f2}, density

$$D_{f2} = - \log T_{f2}$$

Bubbles : exposure E_{b2}, transmission T_{b2}, density $D_{b2} = -\log T_{b2}$

Similarly the ratio of the signal amplitude I_2 to the backround amplitude F_2 is given by :

$$\frac{I_2}{F_2} = \frac{A_b\, (T_{b2} - T_{f2})}{A_s\, T_{f2}} + 1 \qquad (3)$$

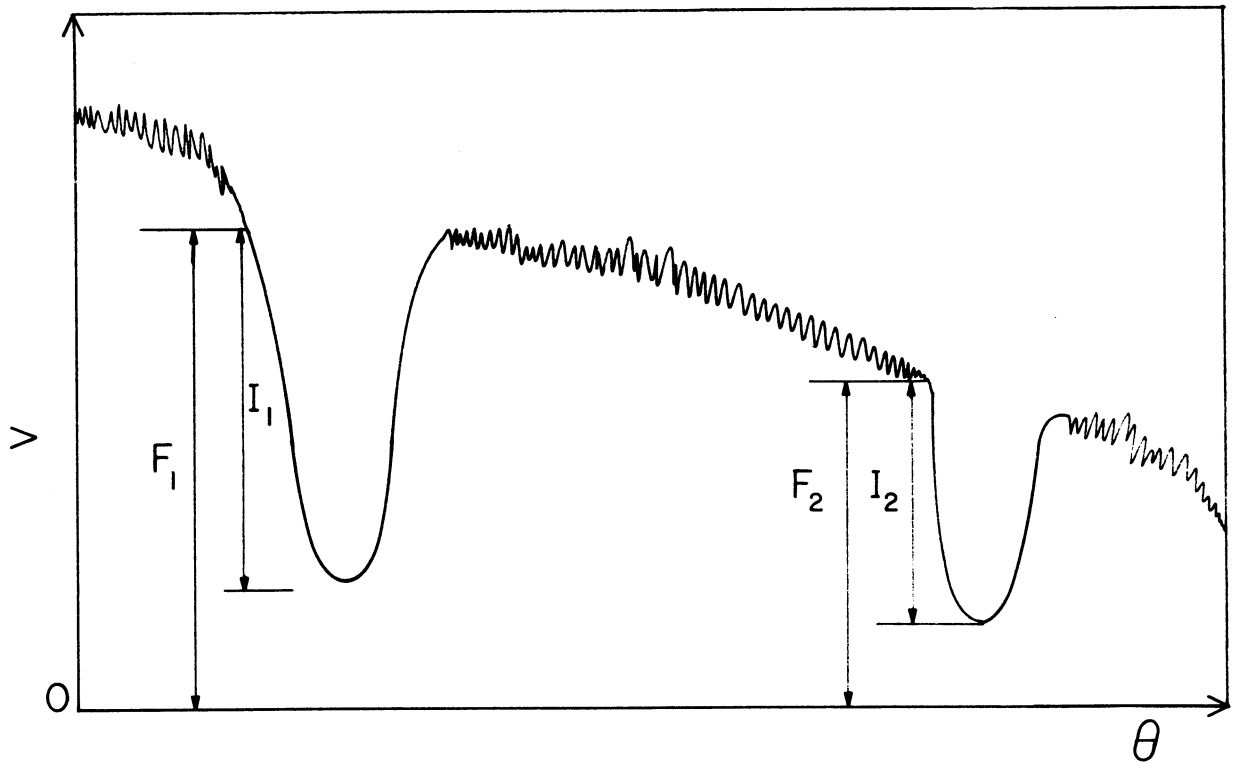

Fig. 5

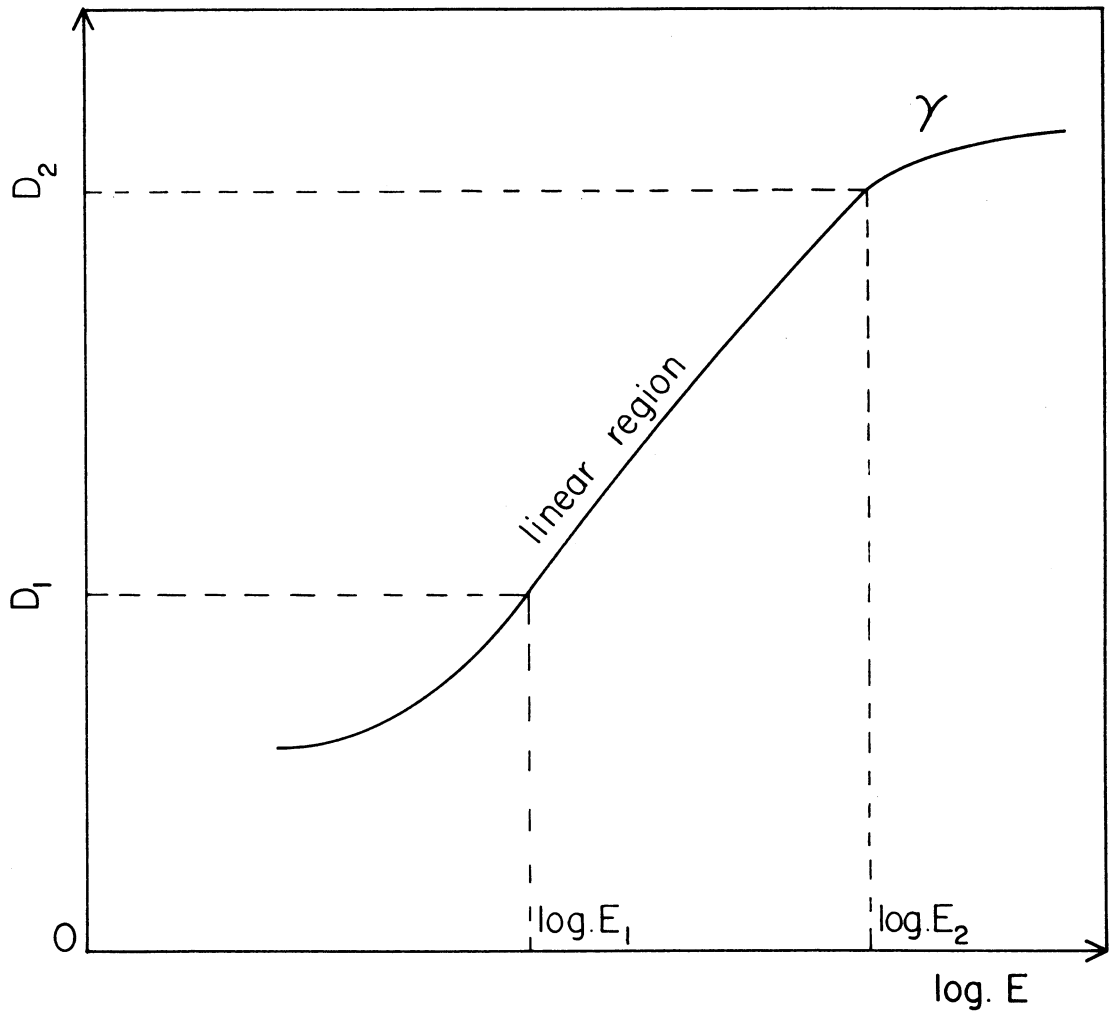

Fig. 6

To obtain a correct signal normalization by the AGC in both conditions, relation (1) must be satisfied, i.e.

$$\frac{A_b\,(T_{b1} - T_{f1})}{A_s\,T_{f1}} + 1 = \frac{A_b\,(T_{b2} - T_{f2})}{A_s\,T_{f2}} + 1 \qquad (4)$$

$$\frac{T_{b1} - T_{f1}}{T_{f1}} = \frac{T_{b2} - T_{f2}}{T_{f2}}$$

$$\frac{T_{b1}}{T_{f1}} = \frac{T_{b2}}{T_{f2}}$$

If we now take the logarithm

$$\log \frac{T_{b1}}{T_{f1}} = \log \frac{T_{b2}}{T_{f2}}$$

$$D_{f1} - D_{b1} = D_{f2} - D_{f1}$$

$$D_{b2} - D_{b1} = D_{f2} - D_{f1}$$

$$\Delta D_b = \Delta D_f \qquad (4')$$

Consider fig. 8 : the slope γ of the curve density versus logarith of exposure is defined as :

$$\gamma = \frac{\Delta D}{\Delta \log E} \qquad (5)$$

If we assume that the chamber is such that

$$E_{b2} = KE_{b1} \qquad E_{f2} = KE_{f1} \qquad (6)$$

Then $$\log \frac{E_{b2}}{E_{b1}} = \log \frac{E_{f2}}{E_{f1}} = \log K = K'$$

$$\log E_{b2} - \log E_{b1} = \log E_{f2} - \log E_{f1}$$

$$\Delta \log E_b = \Delta \log E_f = K' \qquad (6')$$

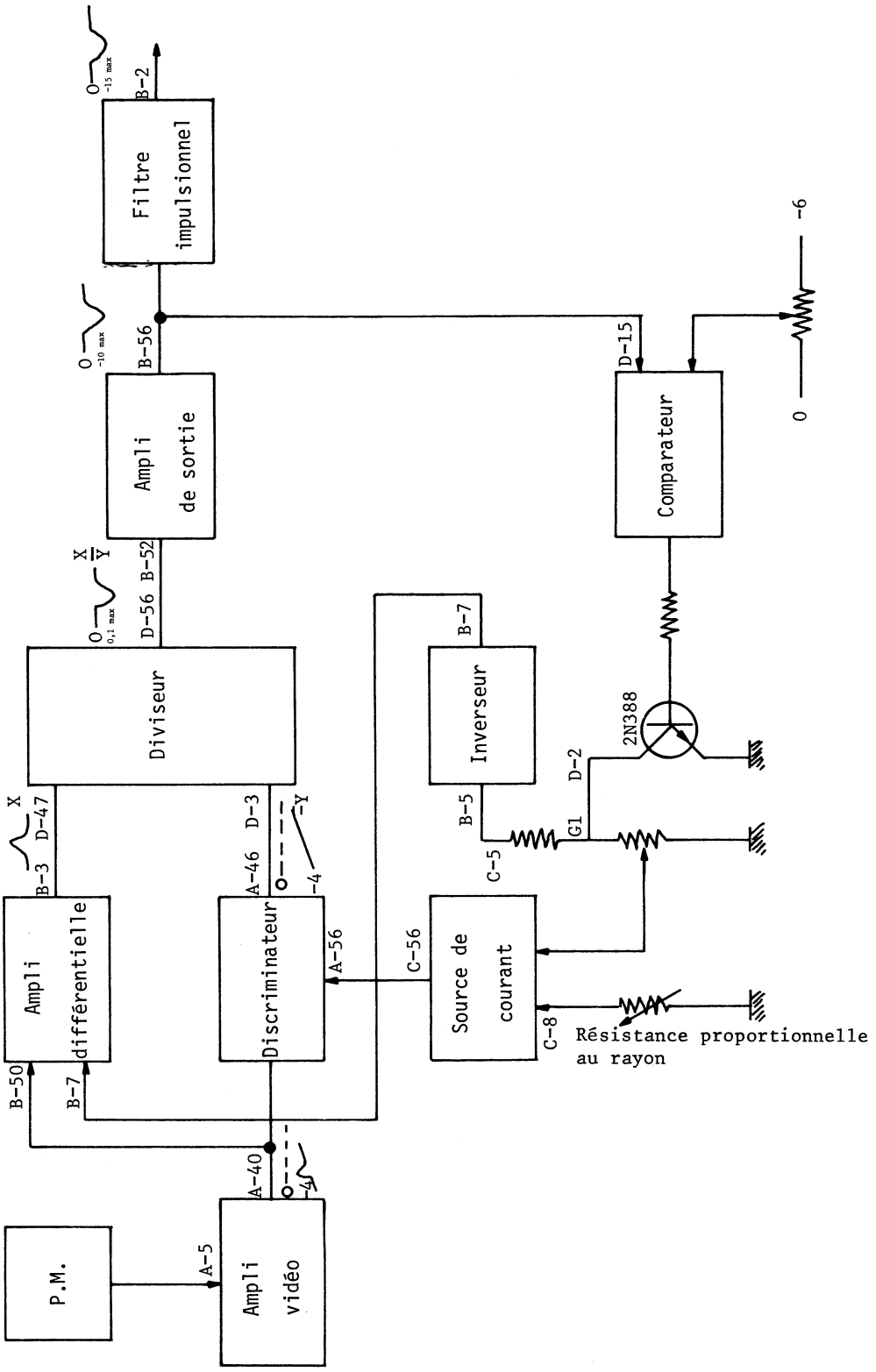
AGC 1
P.M.
A-5
Ampli vidéo
A-40
-4
Ampli différentielle
B-50
B-7
B-3
X
D-47
Diviseur
D-56
B-52
X/Y
Ampli de sortie
B-56
Filtre impulsionnel
B-2
0 -15 max
0 -10 max
0 0,1 max
Discriminateur
A-46
D-3
-Y
-4
A-56
C-56
Source de courant
C-8
Résistance proportionnelle au rayon
Inverseur
B-7
B-5
C-5
G1
D-2
2N388
Comparateur
D-15
-6
0

Fig. 7

AGC 2

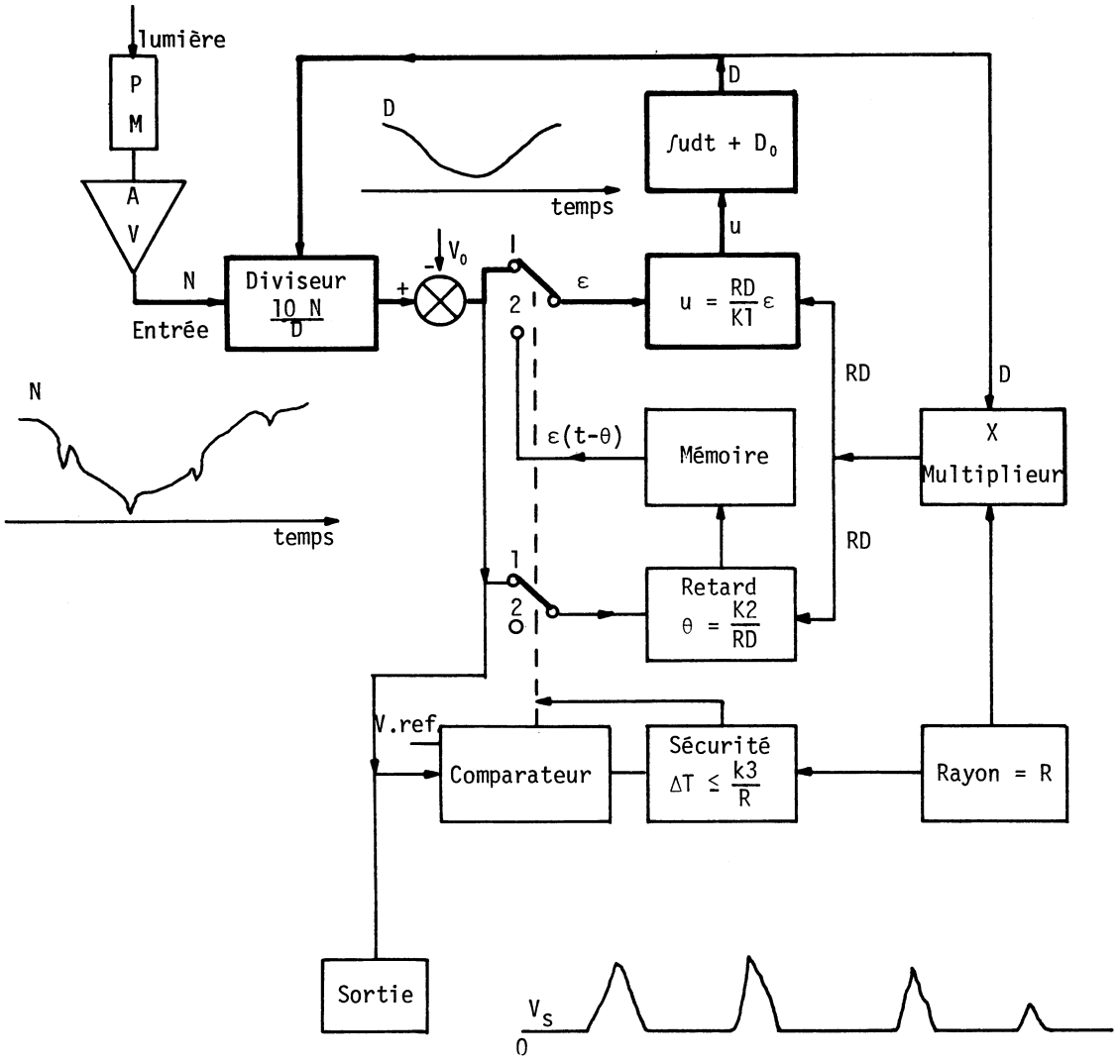
lumière
P
M
A
V
N
Entrée
Diviseur
10 N
D
D
temps
N
temps
+
-
V_0
ε
2
1
$\int udt + D_0$
u
$u = \frac{RD}{K1}\varepsilon$
RD
D
$\varepsilon(t-\theta)$
Mémoire
X
Multiplieur
RD
Retard
$\theta = \frac{K2}{RD}$
V.ref
Comparateur
Sécurité
$\Delta T \leq \frac{k3}{R}$
Rayon = R
Sortie
V_s
0

Fig. 8

Relation (5) applied to the bubbles and to the background gives:

$$\gamma_b = \frac{\Delta D_b}{\Delta \log E_b} \quad \text{and} \quad \gamma_f = \frac{\Delta D_f}{\Delta \log E_f}$$

Introducing (4) and (6) in (7) we obtain.

$$\gamma_b = \gamma_f = \text{const.} \tag{8}$$

If γ_b is different from γ_f or spurious light is not proportional to the backround density, the AGC, is good as it may be, will not be able to correctly perfrom the division in relation (1).

Referring to i) we have tried to protect the slit from the external light, however it was impossible to eliminate all the spurious light so, especially on LSD 2, we have attempted to reduce this effect to a minimum by using a narrow slit and to keep it constant in order to make a software correction possible (ref. 5).

The effect described in ii) may be entirely eliminated by appropriate film exposure and development.

2.2.2 AGCI and AGC2 (figs. 7 and 8)

Due to the fact that the AGCI performances were not entirely satisfactory by ionization measurement (see paper on ionization) AGC2 was designed and mounted on LSD 2.

The following comparison shows the drawbacks of AGCI and the improvements brought by AGC2.

AGCI (ref. 8)	AGC2 (ref. 9)
1. Allows density backround variations in a range of 1 : 10	Allows density backround variations in a range of 1 : 50
2. Performs the I/F division by means of an "open loop" circuit. Precision depends on the variation law of the source driven res resistance of the FET performing the division.	Performs the I/F division by means of a "closed loop" analog divider. The quotient is screwed to a reference value V_o by the feed-back loop.
3. Memorizes a constant value of the backround F, at the pulse detection time. But, during the pulse, the backround slope may be different from zero (fig. 9). In this case the input amplitude will not reach after the pulse, the memorized value. In this case, the pulse detection circuit will not be reset.	Memorizes amplitude and slope of the background. Sums the first one with the integral of the second one. If during the pulse derivative of the background is constant (fig. 10) the denominator F may be considered as following the background slope. In any case, the pulse detection circuit will be reset.

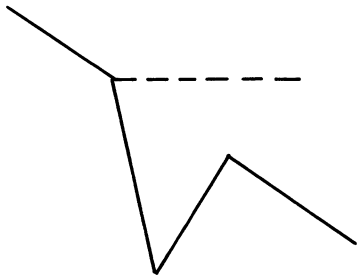

fig. 9

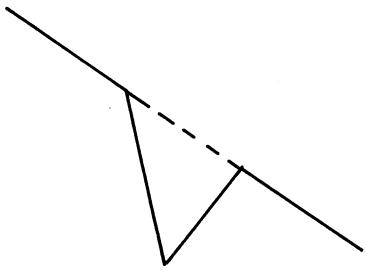

fig. 10

4. Is not equiped with a safety system blocking the discriminator in the case of a step background variation (black flare on the film etc)
5. Its tuning is not easy due to interdependence of the different potentiometers.

Is equiped with a safety system blocking the feedback loop if the pulse width detected is 2-3 times larger than expected. This safety is served to the spiral radius.
Is tuned by 4 independent potentiometers.

Fig. 11 demonstrates the efficiency of AGC 2 versus AGC1.

2.3 ADC circuits on LSD1 and LSD2

2.3.1 Basic principles of LSD1 ADC (fig. 12)

A counter (CTR) controls a Digital to Analog Converter (CDA). An operational amplifier addes the output voltages of the CDA and of the track pulse. The output of this amplifier is given by :

$$S = - K \text{ (CDA output + track PH)}$$

The CDA pulse being positive and the track pulse negative, this amplifier allows to detect the signe of slope variations of the track pulse :

UP → positive output voltage
DOWN → negative output voltage

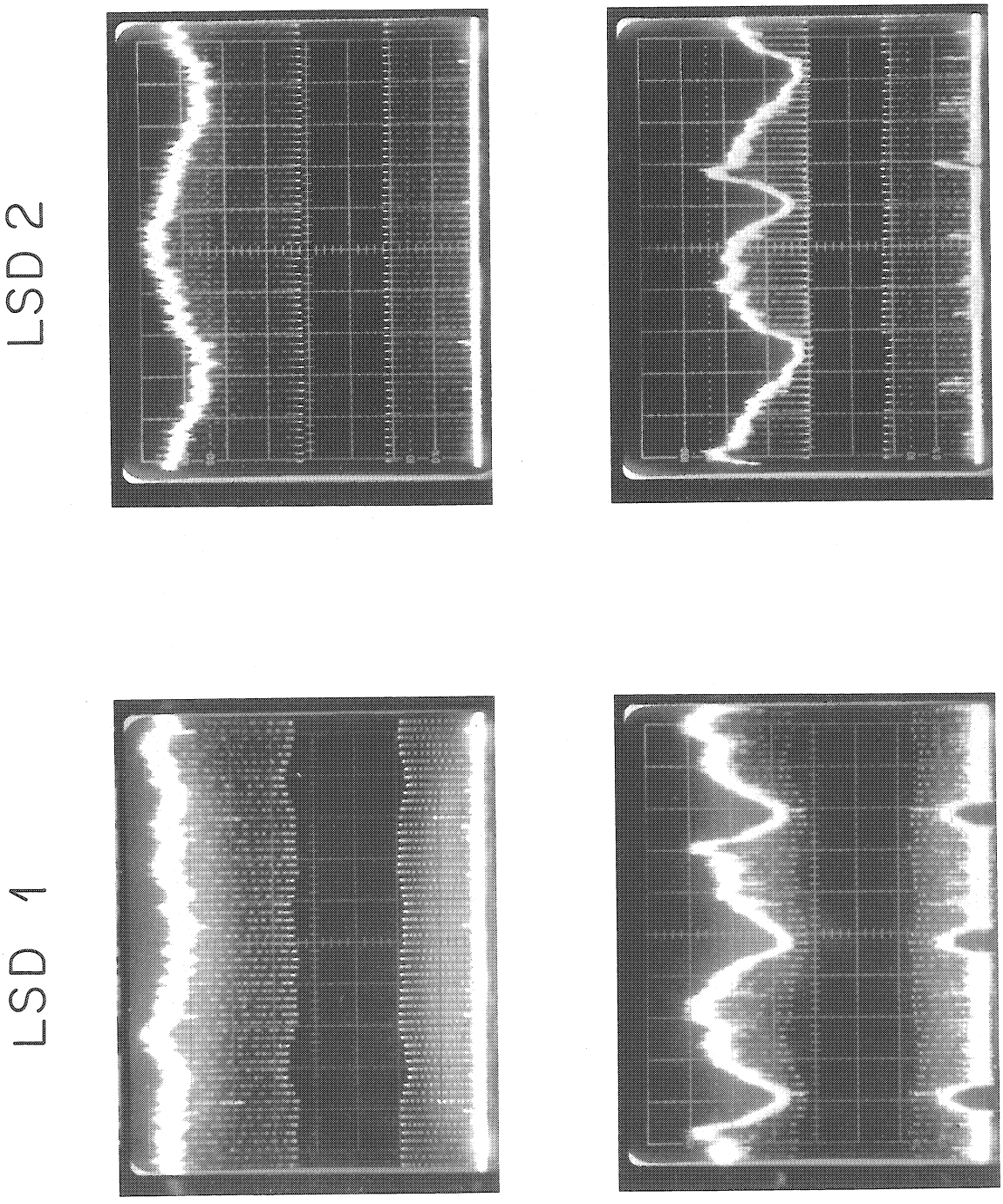

Fig. 11

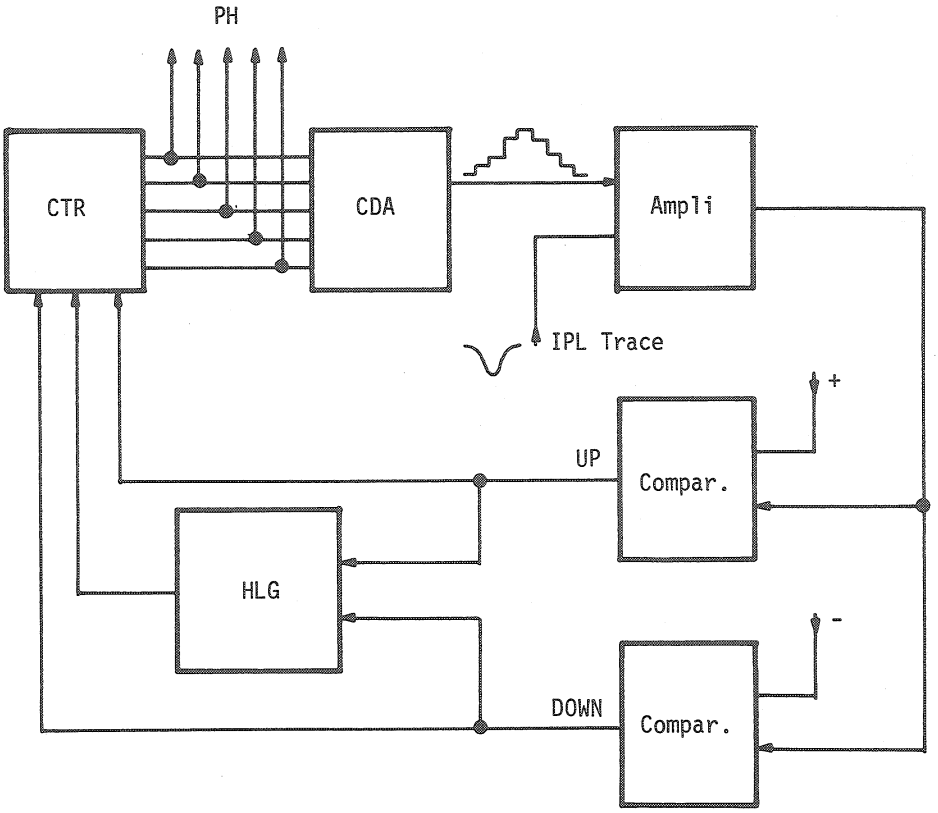

Fig. 12

Two comparators having one a slightly positive and the other a slightly negative reference voltage, assure the shaping of the UP and DOWN signals - These signals control a clock and the signe of the counter increment - Clock gives pulses only in presence of an UP or a DOWN condition -

If there are no track pulses or the two pulses have the same amplitude, the clock is blocked. When several flip-flops of the CTR change state at the same time (for instance when the counter contents goes from 7_8 to 8_8), one hase parasites on the CDA output.

2.3.2 Basic principles of ADC2 (fig. 13)

With the 5 bits giving the PH one can determine a maximum PH value of $37_8 = 31_{10}$; for this reason in this converter we utilize 31 comparators (fig. 14) - Each comparator gives a step of PH.

These comparators receive on "non inverting input" the AGC output and on "inverting input" a reference voltage more or less high according to the rank of the comparator.

The reference voltage is + 5V. Each step will therefore have an amplitude of $\frac{5}{31} \simeq 160$ mV.

We use both the direct and the complemented output of the comparators, in order to realise a decoding giving two square waves A and B (fig. 15), dephased by 90^o, but whose phase changes with UP or DOWN condition :

- decoding $\bar{A}B + A\bar{B}$ gives the weight 2^0
- voltage B gives the weight 2^1
- decoding $(4.\bar{8}) + (12.\bar{1}\bar{6}) + (20.\overline{24}) + 28$ gives the weight 2^2
- decoding $(8.\overline{16}) + 24$ gives the weight 2^3.
- comparator 16 gives directly the weight 2^4.

The detection of the relative position of leading and traiting edges of waves A and B permits to obtain the UP and DOWN conditions as well as the clocks UP and DOWN (figs. 16 and 17).

2.4 Integrator

Let us consider the PH: it is dependent from the angle slit-track, so that the information useful for the ionization is given by the first 13cm in space of the tracks. In order to be independent from this angle, we equipped LSD2 with an integrator, which gives a pulse whose PH is proportional to the area of the AGC pulse (fig. 18).

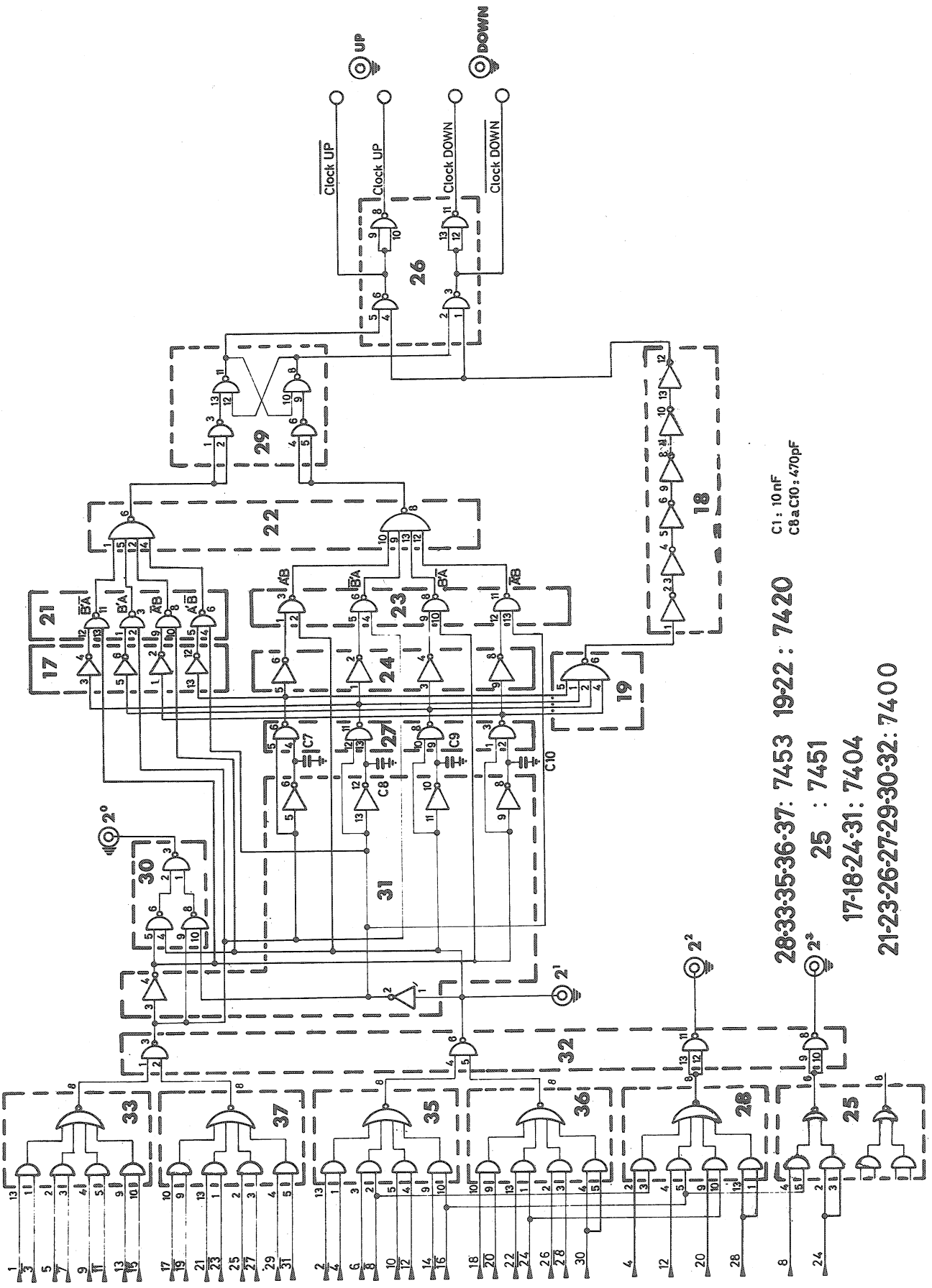
UP
DOWN
Clock UP
Clock UP
Clock DOWN
Clock DOWN
26
29
22
21
17
23
24
19
18
27
C7
C8
C9
C10
C1 : 10nF
C8 a C10 : 470pF
2°
2¹
2²
2³
30
31
32
33
37
35
36
28
25
28-33-35-36-37: 7453 1922 : 7420
25 : 7451
17-18-24-31: 7404
21-23-26-27-29-30-32: 7400

Fig. 13

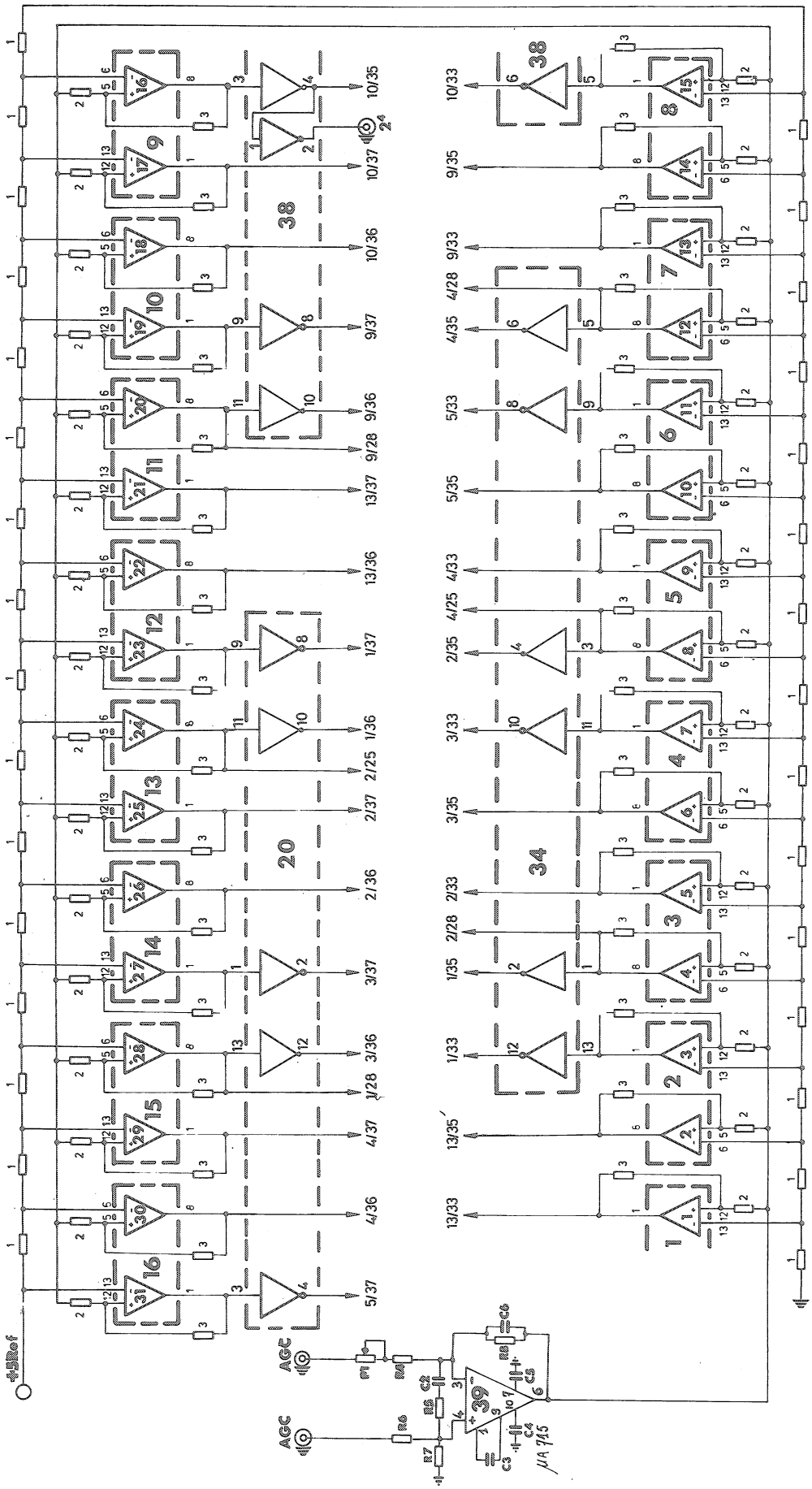
1 a 16 : 72720
20.34.38 : 7404
39 : µA715
C1:10nF
C2:25nF
C3:560pF
C4:1200pF
C5:2200pF
C6:220pF
Resistances "1" 5 Ω 1%
Resistances "2" 1KΩ
Resistances "3" 50KΩ
R4:1K-R5:5.1Ω-R6:5K-R7R8:10K
P1:10K
SN 72720
14 : 3&10
7 : 7&14
+Vref
AGC
AGC
µA 715

Fig. 14

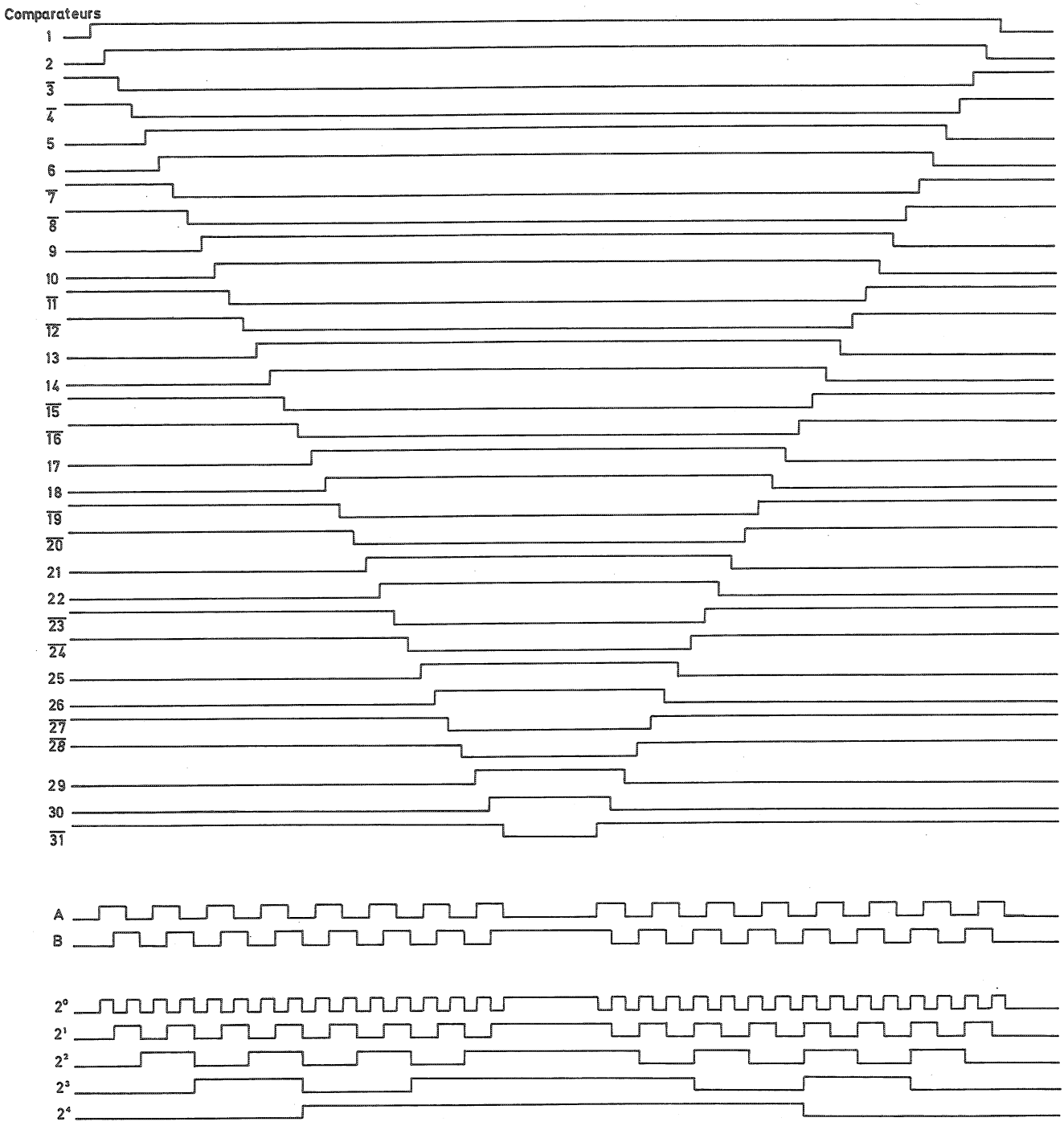

CAD 2

Courbes pour impulsion saturante

Fig. 15

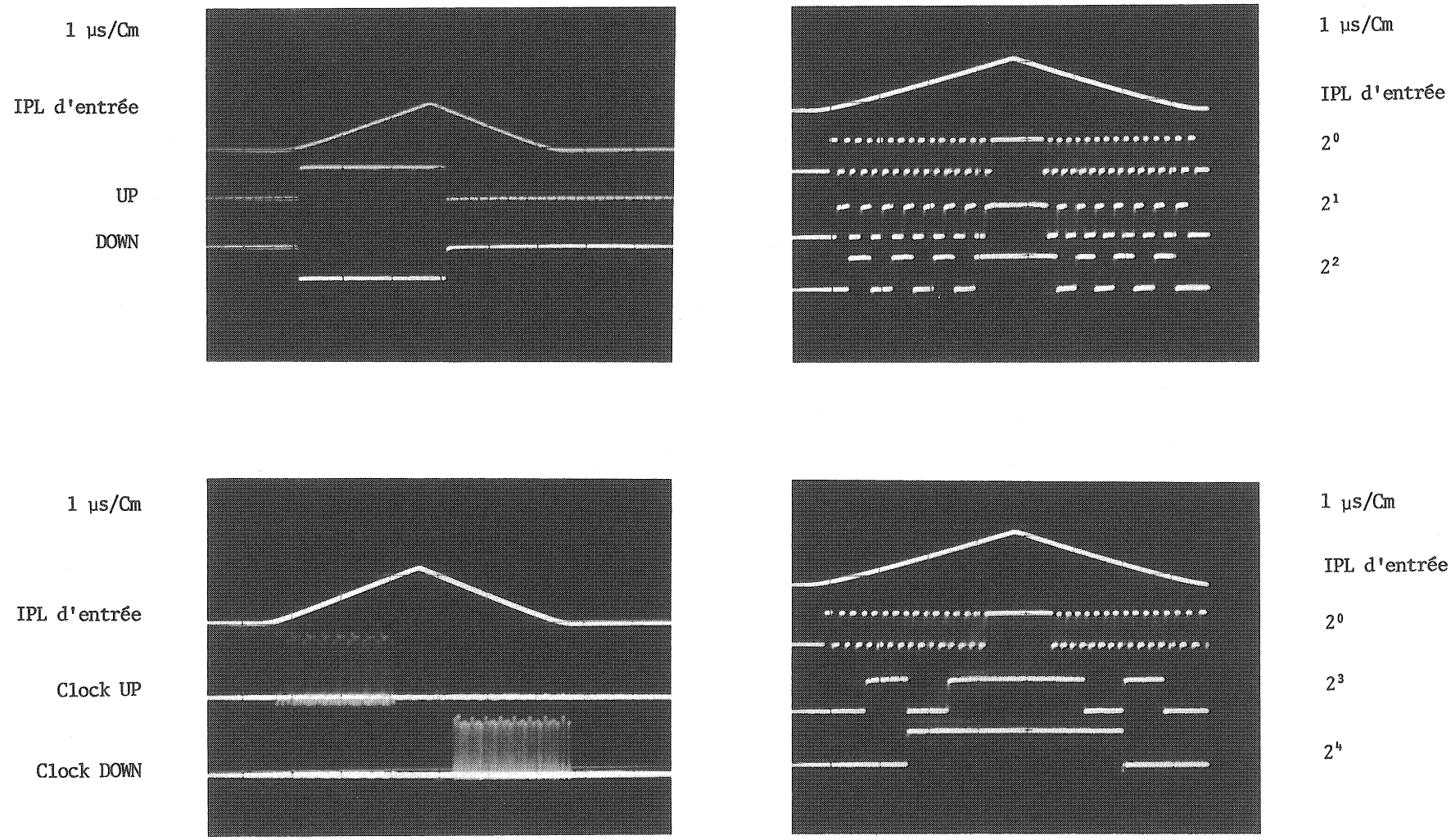
1 µs/Cm
IPL d'entrée
UP
DOWN
1 µs/Cm
IPL d'entrée
2⁰
2¹
2²
1 µs/Cm
IPL d'entrée
Clock UP
Clock DOWN
1 µs/Cm
IPL d'entrée
2⁰
2³
2⁴

Fig. 16

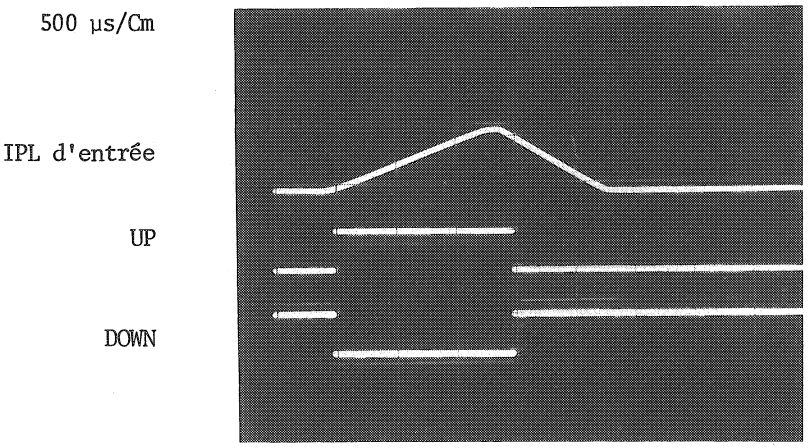
500 µs/Cm
IPL d'entrée
UP
DOWN

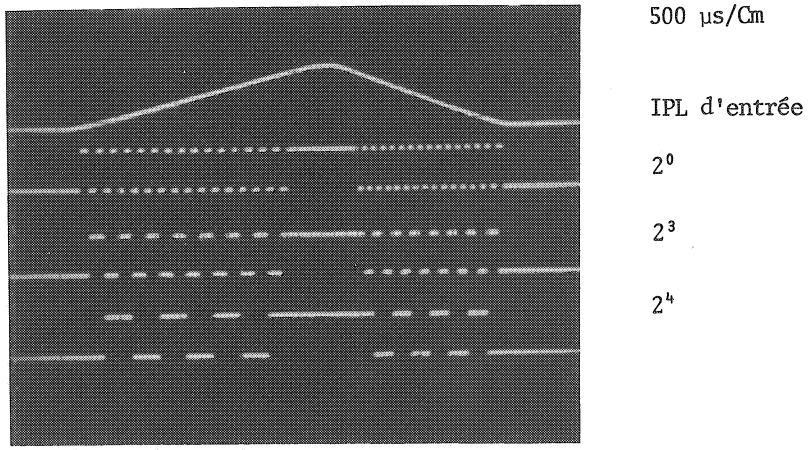
500 µs/Cm
IPL d'entrée
2^0
2^3
2^4

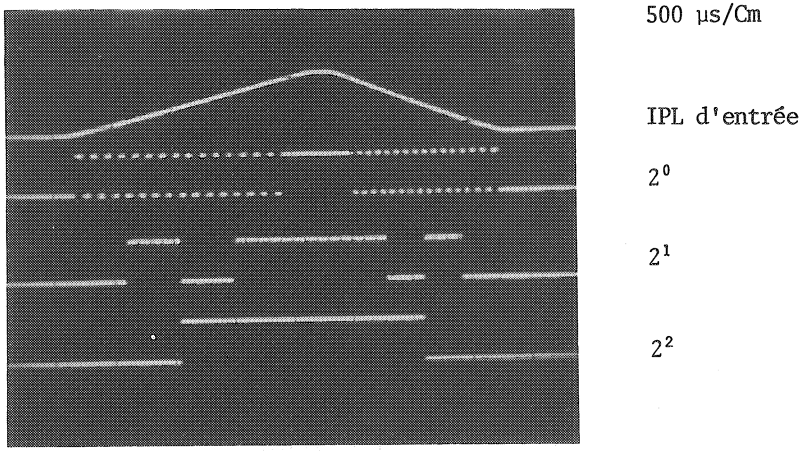
500 µs/Cm
IPL d'entrée
2^0
2^1
2^2

Fig. 17

INTEGRATOR

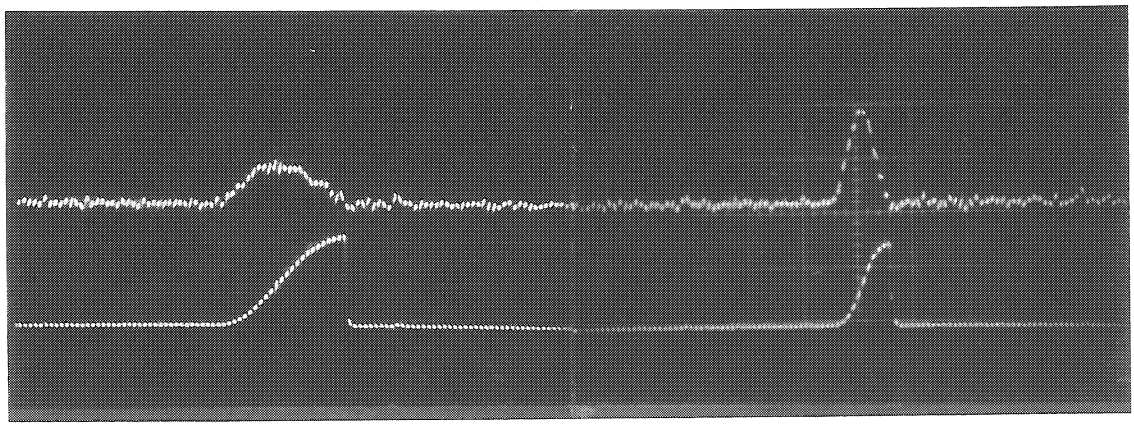

$\alpha \neq 0$ $\alpha = 0$

Fig. 18

REFERENCES

1) P. Wellstead, Raven Data Channel Program, CERN/D.Ph.II/PROG 71-4 Corr., 14 June 1971.

2) E.H. Eichmann, SCALP: The Spiral Reader Calibration Program, CERN/D.Ph.II/PROG 69-2, 25 April, 1969.

3) K.K. Geissler, Some improvements of the LSD Optical System, paper submitted to this Conference.

4) E. Rossa, Réglages Optiques et Mécaniques du LSD et Contrôle de la Qualité des Mesures CERN/D.Ph.II/INSTR 71-8, 25 November 1971.

5) Ph. Gavillet, Measurement and Treatment of Ionisation on CERN LSD1, paper submitted to this Conference.

6) G.V. Butler, Spiral Reader (MPIIIB) System Electronics, description and specification, Lawrence Radiation Laboratory, University of California, UCID 2842, 10 October 1966.

7) E. Rossa, Filtre à Bande Passante asservie au Rayon de la Spirale, CERN/INSTR 71-5, 28 October 1971.

8) D. Boget, G. Reboul, Le Traitement du Signal de Sortie du PM dans le Lecteur en Spirale : Contrôle de gain et discrimination, Collège de France, Laboratoire de Physique Nucléaire, CDF/LSD/68-11, October 1968.

9) S. Reynaud, E. Rossa, Contrôle Automatique de Gain et Normalisation des Impulsions de Sortie sur le Lecteur en Spirale Digitisée, LSD-CERN/INSTR 71-5, 4 Mai 1971.